Third-harmonic generation via nonlinear Raman–Nath diffraction in nonlinear photonic crystal

Yan Sheng,[1,*] Wenjie Wang,[1] Roy Shiloh,[2] Vito Roppo,[3] Ady Arie,[2] and Wieslaw Krolikowski[1]

[1]*Laser Physics Center, Research School of Physics and Engineering, Australian National University, ACT 0200, Australia*

[2]*School of Electrical Engineering, Faculty of Engineering, Tel Aviv University, Tel Aviv 69978, Israel*

[3]*Departament de Fisica i Enginyeria Nuclear, Universitat Politecnica de Catalunya, Rambla Sant Nebridi, 08222 Terrassa, Barcelona, Spain*

**Corresponding author: ysh111@physics.anu.edu.au*

Received June 29, 2011; accepted July 18, 2011;
posted July 21, 2011 (Doc. ID 150145); published August 15, 2011

We report on the observation of multiple third-harmonic conical waves generated in an annular periodically poled nonlinear photonic crystal. We show that the conical beams are formed as a result of the cascading effect involving two parametric processes that satisfy either the transverse and/or longitudinal phase-patching conditions. This is the first experimental observation of third-harmonic generation based on nonlinear Raman–Nath diffraction. © 2011 Optical Society of America

OCIS codes: 190.2620, 190.4410, 220.4000, 050.1940.

Third-harmonic generation (THG, also called frequency tripling) is important in many applications as an effective way to achieve coherent light source at shorter wavelengths. To get efficient THG one often employs a two-step cascaded process that involves successive second-harmonic generation (SHG, $\omega+\omega=2\omega$) and sum-frequency mixing (SFM, $2\omega+\omega=3\omega$) [1]. In a nonlinear photonic crystal (NPC) [2–4], this process can be realized by using the quasi-phase-matching (QPM) technique [5–8] that involves a periodic variation to the sign of the second-order nonlinearity $\chi^{(2)}$ [9]. The resulting modulation enables one to phase-match the constituent processes via a set of reciprocal lattice vectors (RLV), i.e. $\mathbf{k}_2-2\mathbf{k}_1=\mathbf{G}_1$ for SHG and $\mathbf{k}_3-\mathbf{k}_1-\mathbf{k}_2=\mathbf{G}_2$ for SFM, with $\mathbf{k}_l(l=1,2,3)$ being the wave vector of the interacting waves and $\mathbf{G}_{1,2}$ being RLV [10–12]. While these two vectorial relations have been widely used in realization of efficient cascaded THG, it is interesting to see the emission of a third-harmonic (TH) via the so-called Čerenkov-type interaction [13]. The Čerenkov THG represents the type of noncollinear frequency tripling that satisfies only the longitudinal phase-matching conditions: $k_2\cos\theta_1=2k_1$ for SHG and $k_3\cos\theta_2=k_2\cos\theta_1+k_1$ for SFM, with $\theta_{1,2}$ being the Čerenkov angles for the second-harmonic (SH) and TH waves, respectively.

One question is raised whether it is possible to realize cascaded frequency tripling via transverse phase-matching only. It was shown recently that the propagation of a light beam in periodic NPC leads to multiorder diffraction of the SH when the transverse phase-matching condition $k_2\sin\alpha=mG$ (m is integer) is satisfied [14–16], in an analogy to linear Raman–Nath diffraction [17]. Thus, one may expect the nonlinear Raman–Nath diffraction of the TH wave via transverse phase-matched SHG and SFM. However, up until now, only the purely longitudinal (Čerenkov) phase-matched THG was observed [13]. In this Letter we report for the first time on experimental observation of THG which relies on cascaded transverse (Raman–Nath) phase-matching. Moreover, we observe for the first time the THG nonlinear diffraction based on cascading of transverse and longitudinal phase-matched processes. The different phase-matching possibilities provide a set of TH rings at different angles.

The annular NPC was fabricated using electric poling of a Z-cut MgO:doped stoichiometric lithium tantalate (SLT) crystal (thickness 490 μm). The period is 7.5 μm and the duty factor varies inside the sample from 0.7 to 0.8. The domain-inverted structure on the $+Z$-facet of the sample is shown in Fig. 1(a). The fundamental beam from an optical parametric amplifier (Topas), delivering 150 fs pulses at 1.5 μm (repetition rate 250 Hz), propagates along the Z-axis of the sample. The laser is loosely focused to produce a beam waist 100 μm that covers roughly 25 domain periods of the sample. The pump intensity is typically $\sim$60 GW/cm^2.

In Fig. 1(b) we show the observed harmonic pattern in far-field. The simultaneous conical emission of the SH and TH waves is clearly seen. We blocked the center spot of the THG (which is non phase-matched and collinear

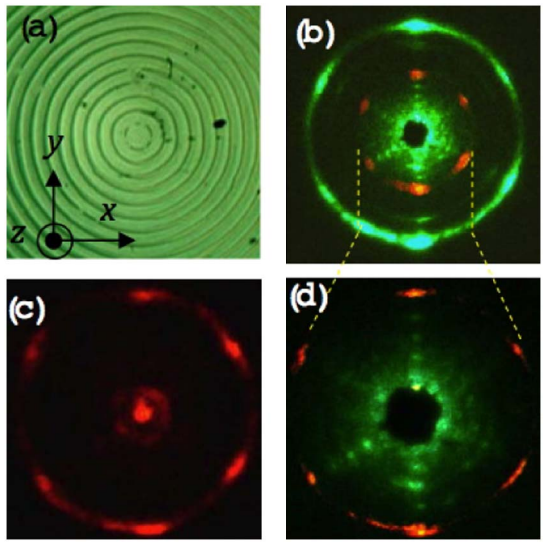

Fig. 1. (Color online) (a) Front facet of the SLT sample with annular domain structure. (b) Far-field image of the SH and TH signal generated via the nonlinear diffraction. (c) and (d) Enlarged section of the SH and TH emission pattern located near the direction of propagation of the fundamental beam.

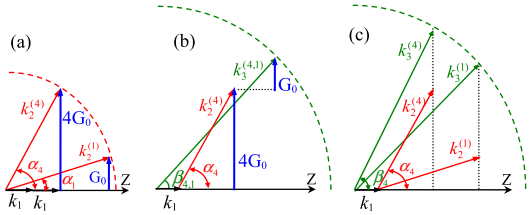

Fig. 2. (Color online) Phase-matching diagrams of (a) Raman–Nath (transverse matching) and Čerenkov (longitudinal matching) SHG; (b) Raman–Nath THG and (c) Čerenkov THG. The angles for the different cases are given in Table 1.

with the fundamental wave) to avoid its scattering on the screen. With the fundamental and TH waves being blocked by suitable filters, an expanded view of the SH emission is displayed in Fig. 1(c). Two SH rings are observed, whereby the inner ring is attributed to the nonlinear Raman-Nath diffraction and the outer ring to the Čerenkov process. The multiple emission of conical TH waves in NPC is observed here for the first time. These TH beams can be classified into two groups according to their propagation angles: (i) central rings surrounding the fundamental beam and always located inside the bigger SH ring [see Fig. 1(d) for an expanded view], and (ii) two peripheral rings, situated relatively far from the fundamental beam. The generation of such TH waves is a result of two-step cascading effect. Their propagation angles, as we will discuss below, agree well with those predicted by the cascading of two parametric processes that are either transversely or longitudinally phase-matched.

To explain the generation of TH rings in details, we consider the phase-matching conditions for the processes of SHG and SFM. For SHG it has been known that the transverse condition $k_2^{(m)} \sin\alpha_m = mG$ leads to the multiorder SHG via nonlinear Raman–Nath diffraction [14,15]. In our case the first- ($m = 1$) and fourth-order ($m = 4$) SHG are observed. Coincidentally, the fourth-order SHG also exactly satisfies the nonlinear Čerenkov radiation condition, i.e. $k_2^{(4)} \cos\alpha_4 = 2k_1$ [18]. The corresponding phase-matching diagram is schematically shown in Fig. 2(a). In a similar way, we analyze the SFM relation by splitting it into the transverse and longitudinal phase-matching conditions:

$$k_3^{(m,n)} \sin\beta_{m,n} = (m+n)G + \Delta k_{3t}, \tag{1}$$

$$k_3^{(m,n)} \cos\beta_{m,n} = k_1 + k_2^{(m)} \cos\alpha_m + \Delta k_{3l}, \tag{2}$$

where $\beta_{m,n}$ is the internal propagation angle of the TH wave, and Δk_{3t}, Δk_{3l} are the phase mismatches in the transverse and longitudinal directions, respectively. In fact, these two scalar relations, as have been verified in experiment, can take effect independently of each other. Note that, for the transverse phase-matching, the SHG depends only on the diffraction order m and the SFM depends only on the order n, while for the longitudinal case, both SH and TH emissions involve only the mth order. Hereafter, we use a single index m for the longitudinally phase-matched TH [$k_3^{(m)}$ and β_m] to distinguish it from the transversely matched TH [$k_3^{(m,n)}$ and $\beta_{m,n}$].

When the transverse phase-matching condition ($\Delta k_{3t} = 0$) is satisfied [Fig. 2(b)], the internal propagation angles of the TH waves can be found from the relation $\sin\beta_{m,n} = (m+n)\lambda_3/n_3\Lambda$, (where n_3 is the TH index of refraction) which can be regarded as the nonlinear Raman–Nath condition governing the diffraction of the TH waves on a NPC. In addition, the efficient THG may also take place under the condition of $\Delta k_{3l} = 0$ [see Fig. 2(c)]. In this case the propagation angle of the TH beam satisfies the relation $\cos\beta_m = (n_1 + 2n_2\cos\alpha_m)/(3n_3)$, depending on the material dispersion as well as the emission angle of the intermediate SHG. In a special case when the intermediate SHG satisfies the Čerenkov SHG condition ($\cos\alpha_m = n_1/n_2$), the emission of the corresponding TH will be determined only by the material dispersion: $\cos\beta_m = n_1/n_3$. This special frequency tripling has been observed as a Čerenkov THG since it relies on the purely longitudinal phase-matching [13].

The discussion so far considered the phase-matching conditions in a single plane. However, since the fundamental beam is incident exactly in the center of the annular structure, the same reasoning applies to any azimuthal angle and consequently the harmonic radiation will appear in the form of concentric cones.

In Table 1 we list measured and predicted propagation angles of the SH and TH waves, using the refractive index data reported in [19]. Good agreement between theory and experiment is evident. The internal three TH rings [group (i)] are generated by cascading two transversely phase-matched parametric processes and hence represent the nonlinear Raman–Nath diffraction of THG. For the peripheral two rings [group (ii)], the internal one is contributed from a transversely phase-matched SHG followed by a longitudinally phase-matched SFM, while the external one is contributed from cascading two longitudinally phase-matched processes and hence represents the Čerenkov THG. Based on our measurements, we

Table 1. The Harmonics and Corresponding Transverse (TPM)/Longitudinal (LPM) Phase-Matching Conditions

Harmonic	Measurement	Theory	Step 1: SHG	Step 2: SFM
SH1[$k_2^{(1)}$]	5.75°	5.74°	$\sin\alpha_1 = \lambda_2/n_2\Lambda$	
SH2[$k_2^{(4)}$]	23.87°	23.89°	$\sin\alpha_4 = 4\lambda_2/n_2\Lambda$	
TH1[$k_3^{(4,-1)}$]	11.51°	11.73°	$k_2^{(4)}$	TPM: $\sin\beta_{4,-1} = (m+n)\lambda_3/n_3\Lambda$, $m = 4$, $n = -1$
TH2[$k_3^{(4,0)}$]	15.64°	15.66°	$k_2^{(4)}$	TPM: $\sin\beta_{4,0} = (m+n)\lambda_3/n_3\Lambda$, $m = 4$, $n = 0$
TH3[$k_3^{(4,1)}$]	19.51°	19.67°	$k_2^{(4)}$	TPM: $\sin\beta_{4,1} = (m+n)\lambda_3/n_3\Lambda$, $m = 4$, $n = 1$
TH4[$k_3^{(1)}$]	33.70°	33.70°	$k_2^{(1)}$	LPM: $\cos\beta_1 = (n_1 + 2n_2\cos\alpha_1)/3n_3$
TH5[$k_3^{(4)}$]	39.30°	39.84°	$k_2^{(4)}$	LPM: $\cos\beta_4 = n_1/n_3$

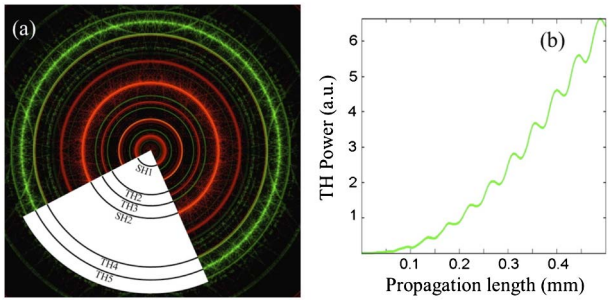

Fig. 3. (Color online) (a) Calculated harmonic emission in the far-field; (b) the TH power growth with the propagation length.

estimated the normalized internal conversion efficiency with respect to the pulse power for the Čerenkov THG $\eta_3^{(4)} = 1.7 \times 10^{-18}\%\,\mathrm{W}^{-2}$ and that for the Raman–Nath interactions of about one order of magnitude lower.

For better verification of our analysis we simulated the emission of the harmonics in the annular $\chi^{(2)}$ structure numerically using split-step Fourier method. Figure 3(a) illustrates the calculated intensity distribution for both harmonics. The agreement between simulations and experimental results is excellent. In simulations, for simplicity, we did not consider the effect of the hexagonal shape of domain structure, which leads to the sixfold modulation of the azimuthal intensity distribution in experiment [18]. In Fig. 3(b), we plot the total TH power as a function of propagation length, in which the coherently growing TH power through the sample represents the typical character of the nonlinear Čerenkov radiation, while its slight fluctuations reflect the contributions from the Raman–Nath harmonics [18].

In conclusion, we have reported on the observation of multiple TH conical waves generated in an annular periodically poled NPC. We have explained the observations by employing the concept of cascaded nonlinear interaction combined with the transverse and longitudinal phase-matching conditions. The TH rings hence represent the cascaded variant of the nonlinear Raman–Nath diffraction and nonlinear Čerenkov radiation. Whereas the angle of the Čerenkov ring is determined solely by the material dispersion, the angle of the Raman–Nath process can be controlled by the nonlinear modulation pattern. Hence, this provides a tool for controlling the angular spectrum of the diffracted TH wave. This phenomena can find application in nonlinear microscopy and nondestructive evaluation of the domain structure in ferroelectric crystals [20]. Moreover, the effects studied here may be also observable in other types of nonlinear physical systems, including, e.g. high-intensity acoustic waves in solids.

This work was supported by the Australian Research Council and the Israel Science Foundation (ISF) (Grant No. 774/09).

References

1. Y. R. Shen, *The Principles of Nonlinear Optics* (Wiley, New York, 1984).
2. V. Berger, Phys. Rev. Lett. **81**, 4136 (1998).
3. N. G. R. Broderick, G. W. Ross, H. L. Offerhaus, D. J. Richardson, and D. C. Hanna, Phys. Rev. Lett. **84**, 4345 (2000).
4. A. Arie and N. Voloch, Laser Photon. Rev. **4**, 355 (2010).
5. J. A. Amstrong, N. Bloembergen, J. Ducuing, and P. S. Pershan, Phys. Rev. **127**, 1918 (1962).
6. M. M. Fejer, G. A. Magel, D. H. Jundt, and R. L. Byer, IEEE J. Quantum Electron. **28**, 2631 (1992).
7. A. Arie, N. Habshoosh, and A. Bahabad, Opt. Quantum Electron. **39**, 361 (2007).
8. Y. Sheng, J. Dou, B. Ma, B. Cheng, and D. Zhang, Appl. Phys. Lett. **91**, 011101 (2007).
9. M. Houe and P. D. Townsend, J. Phys. D **28**, 1747 (1995).
10. S. Zhu, Y. Zhu, and N. Ming, Science **278**, 843 (1997).
11. Y. Sheng, S. M. Saltiel, and K. Koynov, Opt. Lett. **34**, 656 (2009).
12. O. Fister, J. S. Wells, L. Hollberg, L. Zink, D. A. Van Baak, M. D. Levenson, and W. R. Bosenberg, Opt. Lett. **22**, 1211 (1997).
13. Y. Sheng, W. Wang, R. Shiloh, V. Roppo, A. Arie, and W. Krolikowski, Appl. Phys. Lett. **98**, 241114 (2011).
14. S. M. Saltiel, D. N. Neshev, R. Fischer, W. Krolikowski, A. Arie, and Y. S. Kivshar, Phys. Rev. Lett. **100**, 103902 (2008).
15. S. M. Saltiel, D. N. Neshev, W. Krolikowski, A. Arie, O. Bang, and Y. S. Kivshar, Opt. Lett. **34**, 848 (2009).
16. J. Chen and X. Chen, J. Opt. Soc. Am. B **28**, 241 (2011).
17. M. Born and E. Wolf, *Principles of Optics* (Cambridge U. Press, 1999), Chap. 12.
18. S. M. Saltiel, Y. Sheng, N. Bloch, D. N. Neshev, W. Krolikowski, A. Arie, K. Koynov, and Y. S. Kivshar, IEEE J. Quantum Electron. **45**, 1465 (2009).
19. I. Dolev, A. Ganany-Padowicz, O. Gayer, A. Arie, J. Mangin, and G. Gadret, Appl. Phys. B **96**, 423 (2009).
20. Y. Sheng, A. Best, H. Butt, W. Krolikowski, A. Arie, and K. Koynov, Opt. Express **18**, 16539 (2010).